# Measurements of the Exclusive Decays of the $\Upsilon(5S)$ to $B$ Meson Final States and Improved $B_s^*$ Mass Measurement

O. Aquines,[1] Z. Li,[1] A. Lopez,[1] H. Mendez,[1] J. Ramirez,[1] G. S. Huang,[2] D. H. Miller,[2] V. Pavlunin,[2] B. Sanghi,[2] I. P. J. Shipsey,[2] B. Xin,[2] G. S. Adams,[3] M. Anderson,[3] J. P. Cummings,[3] I. Danko,[3] J. Napolitano,[3] Q. He,[4] J. Insler,[4] H. Muramatsu,[4] C. S. Park,[4] E. H. Thorndike,[4] T. E. Coan,[5] Y. S. Gao,[5] F. Liu,[5] R. Stroynowski,[5] M. Artuso,[6] S. Blusk,[6] J. Butt,[6] J. Li,[6] N. Menaa,[6] R. Mountain,[6] S. Nisar,[6] K. Randrianarivony,[6] R. Redjimi,[6] R. Sia,[6] T. Skwarnicki,[6] S. Stone,[6] J. C. Wang,[6] K. Zhang,[6] S. E. Csorna,[7] G. Bonvicini,[8] D. Cinabro,[8] M. Dubrovin,[8] A. Lincoln,[8] D. M. Asner,[9] K. W. Edwards,[9] R. A. Briere,[10] I. Brock,[10,*] J. Chen,[10] T. Ferguson,[10] G. Tatishvili,[10] H. Vogel,[10] M. E. Watkins,[10] J. L. Rosner,[11] N. E. Adam,[12] J. P. Alexander,[12] K. Berkelman,[12] D. G. Cassel,[12] J. E. Duboscq,[12] K. M. Ecklund,[12] R. Ehrlich,[12] L. Fields,[12] R. S. Galik,[12] L. Gibbons,[12] R. Gray,[12] S. W. Gray,[12] D. L. Hartill,[12] B. K. Heltsley,[12] D. Hertz,[12] C. D. Jones,[12] J. Kandaswamy,[12] D. L. Kreinick,[12] V. E. Kuznetsov,[12] H. Mahlke-Krüger,[12] T. O. Meyer,[12] P. U. E. Onyisi,[12] J. R. Patterson,[12] D. Peterson,[12] E. A. Phillips,[12] J. Pivarski,[12] D. Riley,[12] A. Ryd,[12] A. J. Sadoff,[12] H. Schwarthoff,[12] X. Shi,[12] S. Stroiney,[12] W. M. Sun,[12] T. Wilksen,[12] M. Weinberger,[12] S. B. Athar,[13] P. Avery,[13] L. Breva-Newell,[13] R. Patel,[13] V. Potlia,[13] H. Stoeck,[13] J. Yelton,[13] P. Rubin,[14] C. Cawlfield,[15] B. I. Eisenstein,[15] I. Karliner,[15] D. Kim,[15] N. Lowrey,[15] P. Naik,[15] C. Sedlack,[15] M. Selen,[15] E. J. White,[15] J. Wiss,[15] M. R. Shepherd,[16] D. Besson,[17] T. K. Pedlar,[18] D. Cronin-Hennessy,[19] K. Y. Gao,[19] D. T. Gong,[19] J. Hietala,[19] Y. Kubota,[19] T. Klein,[19] B. W. Lang,[19] R. Poling,[19] A. W. Scott,[19] A. Smith,[19] S. Dobbs,[20] Z. Metreveli,[20] K. K. Seth,[20] A. Tomaradze,[20] P. Zweber,[20] J. Ernst,[21] K. Arms,[22] H. Severini,[23] S. A. Dytman,[24] W. Love,[24] S. Mehrabyan,[24] and V. Savinov[24]

(CLEO Collaboration)

[1]*University of Puerto Rico, Mayaguez, Puerto Rico 00681*
[2]*Purdue University, West Lafayette, Indiana 47907, USA*
[3]*Rensselaer Polytechnic Institute, Troy, New York 12180, USA*
[4]*University of Rochester, Rochester, New York 14627, USA*
[5]*Southern Methodist University, Dallas, Texas 75275, USA*
[6]*Syracuse University, Syracuse, New York 13244, USA*
[7]*Vanderbilt University, Nashville, Tennessee 37235, USA*
[8]*Wayne State University, Detroit, Michigan 48202, USA*
[9]*Carleton University, Ottawa, Ontario, Canada K1S 5B6*
[10]*Carnegie Mellon University, Pittsburgh, Pennsylvania 15213, USA*
[11]*Enrico Fermi Institute, University of Chicago, Chicago, Illinois 60637, USA*
[12]*Cornell University, Ithaca, New York 14853*
[13]*University of Florida, Gainesville, Florida 32611, USA*
[14]*George Mason University, Fairfax, Virginia 22030, USA*
[15]*University of Illinois, Urbana-Champaign, Illinois 61801, USA*
[16]*Indiana University, Bloomington, Indiana 47405, USA*
[17]*University of Kansas, Lawrence, Kansas 66045, USA*
[18]*Luther College, Decorah, Iowa 52101, USA*
[19]*University of Minnesota, Minneapolis, Minnesota 55455, USA*
[20]*Northwestern University, Evanston, Illinois 60208, USA*
[21]*State University of New York at Albany, Albany, New York 12222, USA*
[22]*Ohio State University, Columbus, Ohio 43210, USA*
[23]*University of Oklahoma, Norman, Oklahoma 73019, USA*
[24]*University of Pittsburgh, Pittsburgh, Pennsylvania 15260, USA*
(Received 27 January 2006; published 18 April 2006)

Using 420 $\text{pb}^{-1}$ of data collected on the $\Upsilon(5S)$ resonance with the CLEO III detector, we reconstruct $B$ mesons in 25 exclusive decay channels to measure or set upper limits on the decay rate of $\Upsilon(5S)$ into $B$ meson final states. We measure the inclusive $B$ cross section to be $\sigma(\Upsilon(5S) \to B\bar{B}(X)) = (0.177 \pm 0.030 \pm 0.016)$ nb and make the first measurements of the production rates of $\sigma(\Upsilon(5S) \to B^*\bar{B}^*) = (0.131 \pm 0.025 \pm 0.014)$ nb and $\sigma(\Upsilon(5S) \to B\bar{B}^*) = (0.043 \pm 0.016 \pm 0.006)$ nb, respectively. We set 90% confidence level limits of $\sigma(\Upsilon(5S) \to B\bar{B}) < 0.038$ nb, $\sigma(\Upsilon(5S) \to B^{(*)}\bar{B}^{(*)}\pi) < 0.055$ nb and $\sigma(\Upsilon(5S) \to B\bar{B}\pi\pi) < 0.024$ nb. We also extract the most precise value of the $B_s^*$ mass to date, $M(B_s^*) = (5411.7 \pm 1.6 \pm 0.6)$ MeV/$c^2$.

 

DOI: 10.1103/PhysRevLett.96.152001 PACS numbers: 13.25.Gv, 13.66.Bc

The $\Upsilon(5S)$ resonance was discovered by the CLEO [1] and CUSB [2] collaborations. Its production cross section and mass were measured to be about 0.35 nb and $(10.865 \pm 0.008)$ GeV/$c^2$ [1], respectively. Final states can be: $B\bar{B}$, $B\bar{B}^*$, $B^*\bar{B}^*$, $B\bar{B}\pi$, $B\bar{B}^*\pi$, $B^*\bar{B}^*\pi$, $B\bar{B}\pi\pi$, $B_s\bar{B}_s$, $B_s\bar{B}_s^*$, and $B_s^*\bar{B}_s^*$. Here, $B = B_u$ or $B_d$, and the $\pi$ may be charged or neutral (consistent with charge zero of the final state). Throughout this article, we use $B\bar{B}^*$ to signify both $B\bar{B}^*$ and $B^*\bar{B}$. Including a symbol in parentheses indicates that it may or may not be present. The $B$ cross section in this region is well described by the unitarized quark model (UQM) [3], which predicts that about 1/3 of the $b\bar{b}$ decay rate is to $B_s^{(*)}\bar{B}_s^{(*)}$ and that $B^*\bar{B}^*$ dominates the inclusive $B$ rate. A previous CLEO measurement using inclusive $D_s$ production revealed that $\Upsilon(5S) \to B_s^{(*)}\bar{B}_s^{(*)}$ constitutes $(16.0 \pm 2.6 \pm 5.8)\%$ of the total $b\bar{b}$ rate [4]. A second analysis [5], which performed exclusive reconstruction of $B_s$ mesons found $\sigma(e^+e^- \to B_s^*\bar{B}_s^*) = (0.11^{+0.04}_{-0.03} \pm 0.02)$ nb (about 1/3 of the total hadronic resonance cross section). The two results are consistent with each other and with predictions of the UQM.

In this Letter, we measure the contributions of various $B$ meson final states to the $\Upsilon(5S)$ decay. These measurements may better constrain coupled-channel models in the $\Upsilon$ mass region as well as near the lower $\psi$ resonances [6]. We also exploit exclusively reconstructed $B$ mesons from this analysis and the corresponding $B_s$ analysis [5] to extract the most precise measurement of the $B_s^*$ mass to date.

CLEO III is a general purpose solenoidal detector that includes a tracking system for measuring momenta and specific ionization ($dE/dx$) of charged particles, a ring imaging Cherenkov detector (RICH) to aid in particle identification, a CsI calorimeter for detection of electromagnetic showers, and a muon system for identifying muons [7].

The analysis presented here uses 420 pb$^{-1}$ of data collected on the $\Upsilon(5S)$ resonance ($\sqrt{s} = 10.868$ GeV) at the Cornell Electron Storage Ring. Using techniques pioneered at the $\Upsilon(4S)$, we utilize two kinematic variables: the energy difference $\Delta E \equiv E_{\rm beam} - E_B$ and the beam-constrained mass $M_{\rm bc} \equiv \sqrt{E_{\rm beam}^2 - \vec{p}_B^{\,2}}$, where $E_B$ ($\vec{p}_B$) is the energy (momentum) of the reconstructed $B$ candidate and $E_{\rm beam}$ is the beam energy. Because of its low energy, reconstruction of the photon in $B^* \to B\gamma$ is not essential; to maintain high efficiency, we do not reconstruct the $B^*$. (Charge conjugate final states are implied throughout this Letter.)

To obtain a $B$ meson sample of high purity, events are required to have at least five charged tracks and a ratio of the second to zeroth Fox-Wolfram moment [8], $R_2 < 0.25$. Candidate $B$ mesons are reconstructed in exclusive final states containing either $J/\psi$ or $D^{(*)}$ mesons.

Charged particles are required to pass standard selection criteria and are identified by using their measured momenta in conjunction with $dE/dx$, RICH, calorimeter, and muon system information. For particle types $i, j$ ($i, j = \pi, K, p$) we define $\chi^2$-like quantities for $dE/dx$ as the difference in the measured and expected $dE/dx$, normalized by the uncertainty, i.e., $\chi_i^{dE/dx} \equiv (dE/dx_i^{\rm meas} - dE/dx_i^{\rm exp})/\sigma_i$, and for RICH as $\Delta\chi^2_{i,j} \equiv \mathcal{L}_i - \mathcal{L}_j$ (difference in negative log-likelihood between hypotheses $i$ and $j$), respectively. We require at least 3 detected Cherenkov photons from the RICH. Pions are identified by requiring $|\chi_\pi^{dE/dx}| < 4$ or $\Delta\chi^2_{\pi,K} < 5$. For kaons, we define a combined quantity, $\chi^2_{\rm comb} \equiv (\chi_K^{dE/dx})^2 - (\chi_\pi^{dE/dx})^2 + \Delta\chi^2_{K,\pi}$ and require $\chi^2_{\rm comb} < 0$. Electron candidates are formed from particles that have a ratio of calorimeter energy ($E_e$) to measured momentum ($p_e$) in the range $0.5 < E_e/p_e < 1.25$. Muons are identified by either having penetrated at least 3 layers of iron absorber or by having deposited energy in the calorimeter consistent with a minimum ionizing particle ($E < 300$ MeV). Photons are formed from showers that have deposited at least 30 MeV of energy in the calorimeter and are not associated with a charged track. Pairs of photons that have an invariant mass within 2 standard deviations ($\sigma \sim 6$ MeV/$c^2$) of the known $\pi^0$ mass ($M_{\pi^0}$) [9] are defined as $\pi^0$ candidates and are kinematically constrained to give $M_{\pi^0}$.

Candidate $J/\psi$'s are formed from $\mu^+\mu^-$ or $e^+e^-$ pairs. For muon pairs, we require $3.05 < M_{\mu^+\mu^-} < 3.14$ GeV/$c^2$. For $e^+e^-$ combinations with $1.50 < M_{e^+e^-} < 3.14$ GeV/$c^2$, bremsstrahlung photons are searched for among the showers with no matching charged track and within a 5° cone about each electron's initial direction. For each $\mu^+\mu^-$ and $e^+(\gamma)e^-(\gamma)$ candidate, we perform a mass-constrained fit to the $J/\psi$ mass [9] and make a loose requirement that the fit $\chi^2$ per degree of freedom is less than 100. Candidate $\rho^+$ ($K_S^0$) [$K^{*0}$] mesons are formed from $\pi^+\pi^0$ ($\pi^+\pi^-$) [$K^+\pi^-$] combinations that have an invariant mass in the range from 620–920 (490–505) [820–970] MeV/$c^2$. $D^+$ ($D^0$) meson candidates are reconstructed via their decays to $K^-\pi^+\pi^+$ ($K^-\pi^+$, $K^-\pi^+\pi^+\pi^-$, and $K^-\pi^+\pi^0$) and are required to have an invariant mass within $2\sigma$ of their PDG [9] values. To reduce combinatorial background in $D^0 \to K^-\pi^+\pi^0$, we require $p_{\pi^0} > 400$ MeV/$c$. Candidate $D^{*+} \to D^0\pi^+$ ($D^{*+} \to D^+\pi^0$) decays are formed from $D$ and $\pi$ candidates that have a mass difference in the range $144 < M_{D^{*+}} - M_{D^0} < 147$ MeV/$c^2$ ($139 < M_{D^{*+}} - M_{D^+} < 143$ MeV/$c^2$). Similarly, $D^{*0}$ mesons are reconstructed in $D^0\pi^0$, and the mass difference is required to be in the interval $140 < M_{D^{*0}} - M_{D^0} < 144$ MeV/$c^2$.

Candidate $B$ mesons are reconstructed in the 25 decay channels listed in Table I. For $B \to D\rho$ and $B \to D^*\rho$ [10], we take advantage of the helicity angle ($\theta_h$) [11] distribution in these decays and require $|\cos\theta_h| > 0.3$. To improve

TABLE I. Modes used in exclusive $B$ meson reconstruction along with their product branching fractions ($\mathcal{B}_i$) [9], reconstruction efficiencies ($\epsilon_i$), and expected yields ($N^i_{\rm exp}$) in data assuming $\sigma(\Upsilon(5S) \to B\bar{B}(X)) = 0.2$ nb.

| Mode $i$ | $\mathcal{B}_i$ ($10^{-4}$) | $\epsilon_i$ (%) | $N^i_{\rm exp}$ |
|---|---|---|---|
| $B^+ \to J/\psi K^+$ | $1.18 \pm 0.05$ | $43.4 \pm 0.9$ | 4.3 |
| $B^0 \to J/\psi K^{*0}$, $K^{*0} \to K^+\pi^-$ | $1.03 \pm 0.08$ | $25.6 \pm 0.6$ | 2.2 |
| $B^0 \to J/\psi K^0_S$ | $0.34 \pm 0.02$ | $37.2 \pm 1.7$ | 1.1 |
| $B^- \to D^0\pi^-$, $D^0 \to K^-\pi^+$ | $1.87 \pm 0.09$ | $34.4 \pm 0.5$ | 5.4 |
| $B^- \to D^0\pi^-$, $D^0 \to K^-\pi^+\pi^0$ | $6.48 \pm 0.56$ | $12.8 \pm 0.5$ | 7.0 |
| $B^- \to D^0\pi^-$, $D^0 \to K^-\pi^+\pi^+\pi^-$ | $3.67 \pm 0.22$ | $20.7 \pm 0.7$ | 6.4 |
| $B^- \to D^{*0}\pi^-$, $D^{*0} \to D^0\pi^0$, $D^0 \to K^-\pi^+$ | $1.08 \pm 0.11$ | $11.1 \pm 0.5$ | 1.0 |
| $B^- \to D^{*0}\pi^-$, $D^{*0} \to D^0\pi^0$, $D^0 \to K^-\pi^+\pi^0$ | $3.76 \pm 0.47$ | $2.5 \pm 0.2$ | 0.8 |
| $B^- \to D^{*0}\pi^-$, $D^{*0} \to D^0\pi^0$, $D^0 \to K^-\pi^+\pi^+\pi^-$ | $2.13 \pm 0.23$ | $6.9 \pm 0.4$ | 1.2 |
| $B^- \to D^0\rho^-$, $D^0 \to K^-\pi^+$ | $5.11 \pm 0.14$ | $8.2 \pm 0.3$ | 3.5 |
| $B^- \to D^0\rho^-$, $D^0 \to K^-\pi^+\pi^0$ | $17.69 \pm 1.36$ | $3.0 \pm 0.2$ | 4.5 |
| $B^- \to D^0\rho^-$, $D^0 \to K^-\pi^+\pi^+\pi^-$ | $10.02 \pm 0.42$ | $5.2 \pm 0.3$ | 4.4 |
| $B^- \to D^{*0}\rho^-$, $D^{*0} \to D^0\pi^0$, $D^0 \to K^-\pi^+$ | $2.31 \pm 0.42$ | $2.1 \pm 0.1$ | 0.4 |
| $B^- \to D^{*0}\rho^-$, $D^{*0} \to D^0\pi^0$, $D^0 \to K^-\pi^+\pi^0$ | $7.90 \pm 1.54$ | $0.7 \pm 0.1$ | 0.5 |
| $B^- \to D^{*0}\rho^-$, $D^{*0} \to D^0\pi^0$, $D^0 \to K^-\pi^+\pi^+\pi^-$ | $4.56 \pm 0.84$ | $1.5 \pm 0.1$ | 0.6 |
| $B^0 \to D^+\pi^-$, $D^+ \to K^-\pi^+\pi^+$ | $2.64 \pm 0.25$ | $30.9 \pm 1.5$ | 6.9 |
| $B^0 \to D^{*+}\pi^-$, $D^{*+} \to D^0\pi^+$, $D^0 \to K^-\pi^+$ | $0.71 \pm 0.06$ | $22.0 \pm 0.4$ | 1.3 |
| $B^0 \to D^{*+}\pi^-$, $D^{*+} \to D^0\pi^+$, $D^0 \to K^-\pi^+\pi^0$ | $2.47 \pm 0.27$ | $4.0 \pm 0.1$ | 0.8 |
| $B^0 \to D^{*+}\pi^-$, $D^{*+} \to D^0\pi^+$, $D^0 \to K^-\pi^+\pi^+\pi^-$ | $1.40 \pm 0.12$ | $12.2 \pm 0.4$ | 1.4 |
| $B^0 \to D^{*+}\pi^-$, $D^{*+} \to D^+\pi^0$, $D^+ \to K^-\pi^+\pi^+$ | $0.78 \pm 0.08$ | $7.3 \pm 0.5$ | 0.5 |
| $B^0 \to D^+\rho^-$, $D^+ \to K^-\pi^+\pi^+$ | $7.08 \pm 1.28$ | $6.6 \pm 0.4$ | 3.9 |
| $B^0 \to D^{*+}\rho^-$, $D^{*+} \to D^0\pi^+$, $D^0 \to K^-\pi^+$ | $1.75 \pm 0.24$ | $4.3 \pm 0.2$ | 0.6 |
| $B^0 \to D^{*+}\rho^-$, $D^{*+} \to D^0\pi^+$, $D^0 \to K^-\pi^+\pi^0$ | $6.08 \pm 0.93$ | $1.3 \pm 0.1$ | 0.7 |
| $B^0 \to D^{*+}\rho^-$, $D^{*+} \to D^0\pi^+$, $D^0 \to K^-\pi^+\pi^+\pi^-$ | $3.44 \pm 0.48$ | $2.7 \pm 0.2$ | 0.8 |
| $B^0 \to D^{*+}\rho^-$, $D^{*+} \to D^+\pi^0$, $D^+ \to K^-\pi^+\pi^+$ | $1.94 \pm 0.29$ | $1.7 \pm 0.1$ | 0.3 |
| Total | $\sum \mathcal{B}_i\epsilon_i = 7.2 \times 10^{-4}$ | | 60.4 |

the signal-to-background ratio, we also reject low momentum (backward-emitted) $\pi^0$'s from the $\rho^+$ decays by requiring $\cos\theta_h > -0.7$. Table I also shows the product branching fractions, $\mathcal{B}_i$, including the branching ratios of the daughter modes [9], and the reconstruction efficiencies, $\epsilon_i$ determined from Monte Carlo simulations [12–14] of these decays followed by a GEANT [15] based detector simulation. We validate our simulation and analysis procedure by measuring branching fractions for these decay modes using data collected on the $\Upsilon(4S)$ resonance. Good agreement with the world averages are found for all modes.

We first determine the total $B$ meson yield by fitting the invariant mass distribution formed from candidates in the $M_{\rm bc}$, $\Delta E$ region of $5.272 < M_{\rm bc} < 5.448$ GeV/$c^2$, $-0.2 < \Delta E < 0.45$ GeV. The relatively wide $\Delta E$ region is used to avoid biasing the background shape. The invariant mass distribution, shown in Fig. 1, is fit to the sum of a second-order polynomial background and a Gaussian signal shape whose width is fixed to 12.3 MeV/$c^2$, the expected average resolution of these candidates. We find a yield of $53.2 \pm 9.0$ events; fitting to the $J/\psi$ and $D^{(*)}$ distributions individually results in $11.2 \pm 3.5$ and $42.3 \pm 8.4$ $D^{(*)}$ events, respectively. Using $\sum \mathcal{B}_i\epsilon_i = 7.2 \times 10^{-4}$ (see Table I), we measure a cross section $\sigma(\Upsilon(5S) \to B\bar{B}(X)) = (0.177 \pm 0.030)$ nb.

Figure 2 shows the reconstructed events in the $M_{\rm bc} - \Delta E$ plane for $\Upsilon(5S)$ data. Signal and sideband regions are defined using MC simulations of these final states. To extract rates for $B\bar{B}$, $B\bar{B}^*$, and $B^*\bar{B}^*$ separately, we select events in a signal region defined by the area between the diagonals $M_{\rm bc} = 1.018\Delta E + 5.248$ GeV/$c^2$ and $M_{\rm bc} = 1.018\Delta E + 5.312$ GeV/$c^2$. This restricted signal region has a total $\sum \mathcal{B}_i\epsilon_i = 5.7 \times 10^{-4}$. Lower and upper sidebands of the same $\Delta E$ width, also shown in Fig. 2, are shifted to the left and right of the signal region by 10 MeV, respectively.

The $B\bar{B}$, $B\bar{B}^*$, and $B^*\bar{B}^*$ final states are kinematically well separated, but $B^{(*)}\bar{B}^{(*)}\pi$ final states have a large degree of overlap, and with the limited statistics cannot be distinguished. The $B\bar{B}\pi\pi$ final states, because of the limited phase space, peak at $M_{\rm bc} \simeq E_{\rm beam}$. If their rate is large enough, their shape (in $M_{\rm bc}$) will be sufficient to distinguish them from the broad tail of $B^{(*)}\bar{B}^{(*)}\pi$ final states that extend into the $M_{\rm bc}$ region of $B\bar{B}\pi\pi$.

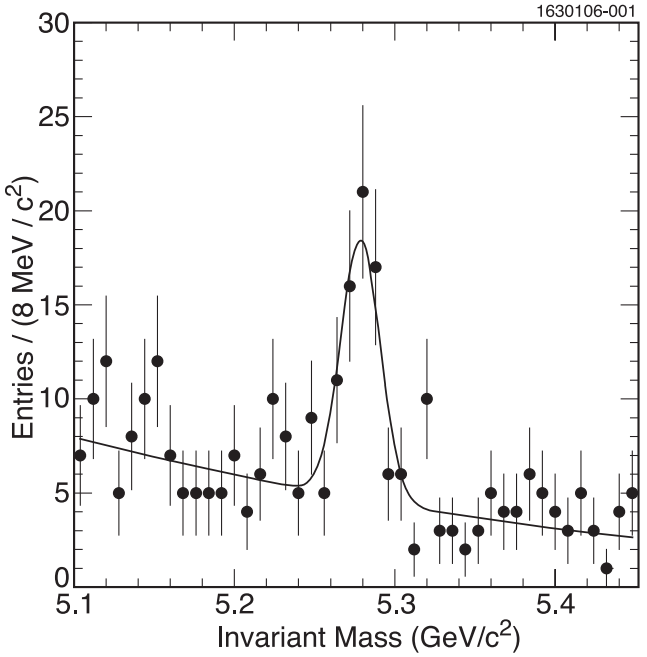


FIG. 1. The $B$ meson invariant mass distribution for all $B$ decay modes listed in Table I in the $\Upsilon(5S)$ data. The points are the data and the curve is the fit described in the text.

Events in the signal region of Fig. 2 are projected onto the $M_{\rm bc}$ axis (see Fig. 3) and fit to the sum of a flat background and three Gaussian signals, one each for the $M_{\rm bc}$ peaks produced by $B\bar{B}$, $B\bar{B}^*$, and $B^*\bar{B}^*$ events. The signal resolutions are set to $\sigma = 4.0$, 6.2, and 7.0 MeV$/c^2$, respectively, as determined from Monte Carlo (MC) simulation, and the background is fixed to 0.7 events/4 MeV, as determined from the average of the upper and lower sidebands. In the fit we use the precisely known mass difference $M_{B^*} - M_B$ [9] and constrain its value to 47.5 MeV$/c^2$ [16]. The middle peak, which corresponds to $\Upsilon(5S) \to B\bar{B}^*$, is not constrained in the fit and is found to be within $1\sigma$ of the expected value.

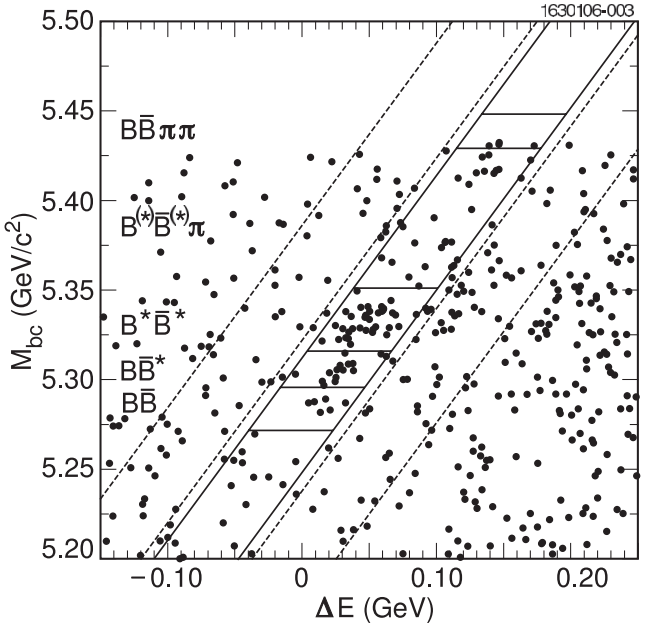


FIG. 2. Scatter plots of $M_{\rm bc}$ vs $\Delta E$ for all $B$ decay modes listed in Table I in the $\Upsilon(5S)$ data. The diagonal lines show the expected signal (solid) and 2 sideband (dashed) regions, as discussed in the text. The horizontal lines show the regions for the various $B\bar{B}(X)$ final states.

The fitted yields are $3.7^{+3.1}_{-2.4}$ $B\bar{B}$, $10.3 \pm 3.9$ $B\bar{B}^*$, and $31.4 \pm 6.1$ $B^*\bar{B}^*$ events. Only the latter two are statistically significant with significances, determined from the change in log-likelihood when the contribution from each peak is removed, of $4.3\sigma$ and $7.6\sigma$, respectively. For $B\bar{B}$, we compute an upper limit of 7.5 events at 90% confidence level (C.L.). A potential excess in $B^{(*)}\bar{B}^{(*)}\pi$ is examined by plotting the invariant mass of candidates in the $B^{(*)}\bar{B}^{(*)}\pi$ region defined by $5.351 < M_{\rm bc} < 5.429$ GeV$/c^2$ and $-0.2 < \Delta E < 0.45$ GeV, which should exhibit a peak at $M_B$ (see inset in Fig. 3). This $M_{\rm bc} - \Delta E$ region includes $(88 \pm 6)\%$ of reconstructed $B^{(*)}\bar{B}^{(*)}\pi$ events, where the uncertainty reflects the maximum variation based on the possible $B^{(*)}\bar{B}^{(*)}\pi$ final states. That distribution is fit to the sum of a Gaussian signal whose mean and rms width are constrained to 5.279 GeV$/c^2$ and 12.3 MeV$/c^2$, respectively, and a linear background shape. The yield of $6.7^{+5.1}_{-4.5}$

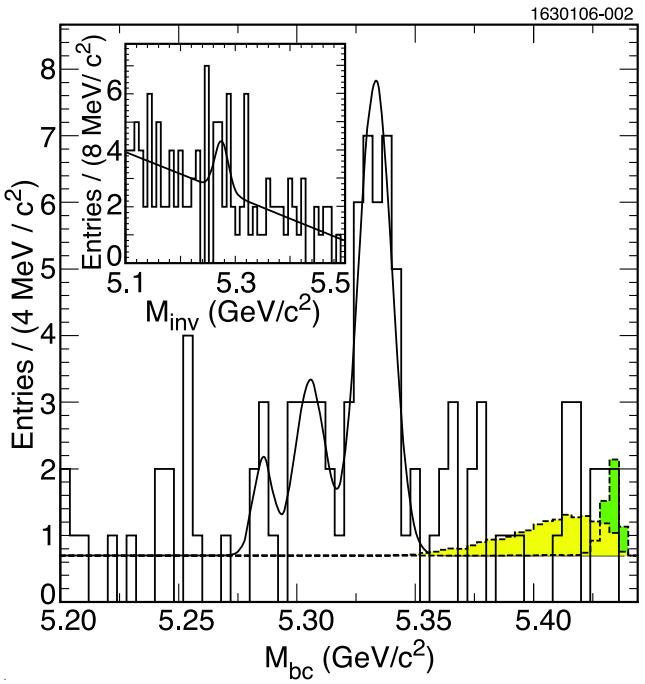


FIG. 3 (color online). Distribution of $M_{\rm bc}$ for all reconstructed $B$ modes listed in Table I for the $\Upsilon(5S)$ data. The histogram displays the data, the curve shows the fit described in the text and the flat line shows the background as determined from a fit to the sidebands as discussed in the text. Distributions for $B^{(*)}\bar{B}^{(*)}\pi$ (lightly shaded) and $B\bar{B}\pi\pi$ (darker shading) obtained from MC simulation of these final states are superimposed for illustrative purposes. The inset shows the invariant mass of candidates in the $B^{(*)}\bar{B}^{(*)}\pi$ $M_{\rm bc}$ region with the fit superimposed.

is not statistically significant, and we compute an upper limit of 13.1 events at 90% C.L.

For the $B\bar{B}\pi\pi$ final state, we select events in the region $5.429 < M_{\rm bc} < E_{\rm beam}$ GeV/$c^2$ and $-0.2 < \Delta E < 0.45$ GeV and find three events consistent with $M_B$. This additional requirement on $M_{\rm bc}$ and $\Delta E$ has an efficiency of $(95 \pm 2)\%$. While the combinatorial background is small ($\sim 0.3$ events), the crossfeed from $B^{(*)}\bar{B}^{(*)}\pi$ into the $B\bar{B}\pi\pi$ signal region is $(12 \pm 6)\%$. If we conservatively assume a $B^{(*)}\bar{B}^{(*)}\pi$ yield equal to its 90% upper limit value and that the $3 B\bar{B}\pi\pi$ candidates are also $B^{(*)}\bar{B}^{(*)}\pi$, we would expect 1.0–2.9 $B^{(*)}\bar{B}^{(*)}\pi$ events to lie within the $B\bar{B}\pi\pi$ mass region. Based on this range of expected background and 3 observed events, we take the most conservative upper limit on $\Upsilon(5S) \to B\bar{B}\pi\pi$, which corresponds to 6.4 [17] events at 90% C.L. For illustration, we superimpose on Fig. 3, $6.7 B^{(*)}\bar{B}^{(*)}\pi$ (lightly shaded, with a ratio of 1:1:1 for $B^*\bar{B}^*\pi$:$B\bar{B}^*\pi$:$B\bar{B}\pi$) and $3 B\bar{B}\pi\pi$ (darker shading) events. Yields, efficiencies, cross sections, and relative production fractions are summarized in Table II. We also show the cross sections as determined from the $J/\psi$ and $D^{(*)}$ modes separately. We find that $B^*\bar{B}^*$ is indeed dominant, comprising $(74 \pm 15)\%$ of the $B\bar{B}(X)$ rate.

Several sources of systematic uncertainty on the cross sections' measurements are considered. Potential errors from the background normalization and shape are evaluated by using different background parametrizations and varying the normalization within its uncertainty. The corresponding uncertainties in the cross sections vary from 3.1% for $\Upsilon(5S) \to B\bar{B}(X)$ to 16.7% for $B\bar{B}$. Uncertainties in the reconstruction efficiencies include contributions from charged particle tracking and identification, $K_s^0$ and $\pi^0$ reconstruction, and finite MC statistics. Averaged over all modes, we find an uncertainty of 6.5%. The analysis procedure was also checked by comparing $B$-meson branching fractions in our signal modes measured using data collected on the $\Upsilon(4S)$ resonance with PDG values [9]. We find a relative difference of $(1 \pm 3)\%$, averaged over all modes, indicating that the efficiencies are well understood. Errors due to the fixed signal shape parameters are determined by varying them within their uncertainties and refitting (3%–4%). The occurrence of multiple candidates in data (in a single event) are found to agree with simulation to within 3%. Uncertainties on input branching fractions and measured integrated luminosity contribute 3% and 2%, respectively. These systematic uncertainties are added in quadrature and the resulting values are included in the cross sections shown in Table II.

We proceed to use the $M_{\rm bc}$ distribution from this analysis in combination with the one for $B_s^*$ in Ref. [5] to obtain an improved measurement of the $B_s^*$ mass. Since those results used exactly the same data set as in this analysis, the largest systematic error, the beam energy calibration of $(+4.6 \pm 2.9)$ MeV [5], cancels out in the (uncorrected) $M_{\rm bc}$ difference, $M_{\rm bc}(B_s^*) - M_{\rm bc}(B^*)$. The rightmost peak in Fig. 3 corresponds to $\Upsilon(5S) \to B^*\bar{B}^*$, and its mean value is measured to be $(5333.1 \pm 1.3(\text{stat}))$ MeV/$c^2$. The $M_{\rm bc}$ peak value for $\Upsilon(5S) \to B_s^*\bar{B}_s^*$ from Ref. [18] is $(5418.2 \pm 1.0 \pm 3.0)$ MeV, where we have added back the $(+4.6 \pm 2.9)$ MeV beam energy correction to obtain an uncorrected value. The difference in the $M_{\rm bc}$ peak values, $M_{\rm bc}(B_s^*\bar{B}_s^*) - M_{\rm bc}(B^*\bar{B}^*)$, can be translated into the mass difference, $M(B_s^*) - M(B^*)$ after correcting for the $-1.7(-0.1)$ MeV/$c^2$ bias that is introduced due to our use of reconstructed $B_{(s)}$ instead of $B_{(s)}^*$ mesons. We therefore find a mass difference $M(B_s^*) - M(B^*) = (86.7 \pm 1.6 \pm 0.2)$ MeV/$c^2$. The 1.6 MeV/$c^2$ error is statistical and the 0.2 MeV/$c^2$ uncertainty is from systematic errors in fitting our $M_{\rm bc}$ spectrum. Combining this mass difference with $M(B^*) = (5325.0 \pm 0.6)$ MeV/$c^2$ [9], we obtain an improved value for the $B_s^*$ mass, $M(B_s^*) = (5411.7 \pm 1.6 \pm 0.6)$ MeV/$c^2$. Using the well-measured $B_s$ mass from CDF of $M(B_s) = (5366.01 \pm 0.73 \pm 0.33)$ MeV/$c^2$ [19], we determine the $1^- - 0^-$ mass splitting $M(B_s^*) - M(B_s) = (45.7 \pm 1.7 \pm 0.7)$ MeV/$c^2$. This mass splitting measurement supersedes the previous CLEO result [5] of $(48 \pm 1 \pm 3)$ MeV/$c^2$ [5] and is significantly more precise than an earlier indirect measurement of $(47.0 \pm 2.6)$ MeV/$c^2$ [20]. It is also consistent with the corresponding splitting in the $B_d$ system of $(45.78 \pm 0.35)$ MeV/$c^2$ [9] as expected from heavy-quark symmetry [21].

In summary, we have measured or set upper limits on the rates for the various final states in $\Upsilon(5S)$ decay. We find

TABLE II. Summary of yields, efficiencies, cross sections, and fractional contributions of various subprocesses in $\sigma(\Upsilon(5S) \to B\bar{B}(X))$ decays. Upper limits are set at the 90% C.L. Uncertainties are from statistical and systematic sources, respectively.

| $\Upsilon(5S) \to$ | Yield (#Events) | Efficiency ($10^{-4}$) | Cross Section (nb) | $\sigma/\sigma(\Upsilon(5S) \to B\bar{B}(X))$ (%) |
|---|---|---|---|---|
| $B\bar{B}$ | $<7.5$ | $5.7 \pm 0.4$ | $<0.038$ | 22 |
| $B^*\bar{B}$ | $10.3 \pm 3.9$ | $5.7 \pm 0.4$ | $0.043 \pm 0.016 \pm 0.006$ | $24 \pm 9 \pm 3$ |
| $B^*\bar{B}^*$ | $31.4 \pm 6.1$ | $5.7 \pm 0.4$ | $0.131 \pm 0.025 \pm 0.014$ | $74 \pm 15 \pm 8$ |
| $B^{(*)}\bar{B}^{(*)}\pi$ | $<13.1$ | $6.3 \pm 0.6$ | $<0.055$ | $<32$ |
| $B\bar{B}\pi\pi$ | $<6.4$ | $6.8 \pm 0.5$ | $<0.024$ | $<14$ |
| $\sigma(\Upsilon(5S) \to B\bar{B}(X))$ | $53.2 \pm 9.1$ | $7.2 \pm 0.5$ | $0.177 \pm 0.030 \pm 0.016$ | |
| $J/\psi$ Modes | $11.2 \pm 3.5$ | $6.3 \pm 0.5$ | $0.295 \pm 0.092 \pm 0.028$ | |
| $D^{(*)}$ Modes | $42.3 \pm 8.4$ | $0.9 \pm 0.1$ | $0.161 \pm 0.032 \pm 0.015$ | |

that predictions of the UQM [3] are consistent with our findings that $B^*\bar{B}^*$ is dominant, with a measured value of $(74 \pm 15)\%$ of the total $B$ rate. The $B\bar{B}^*$ rate is measured to be about $1/3$ of the $B^*\bar{B}^*$ rate. Upper limits on $B\bar{B}$, $B^{(*)}\bar{B}^{(*)}\pi$ and $B\bar{B}\pi\pi$ have also been presented. Lastly, we utilized the $M_{\rm bc}$ peak positions for $B^*$ and $B_s^*$ [5] to extract $M(B_s^*) = (5411.7 \pm 1.6 \pm 0.6)\ \mathrm{MeV}/c^2$, which is the most precise value of the $B_s^*$ mass to date.

We gratefully acknowledge the effort of the CESR staff in providing us with excellent luminosity and running conditions. This work was supported by the A. P. Sloan Foundation, the National Science Foundation, and the U.S. Department of Energy.

*Present address: Universität Bonn, Nussallee 12, D-53115 Bonn, Germany.

[1] D. Besson *et al.* (CLEO Collaboration), Phys. Rev. Lett. **54**, 381 (1985).
[2] D. M. Lovelock *et al.* (CUSB Collaboration), Phys. Rev. Lett. **54**, 377 (1985).
[3] N. Törnqvist, Phys. Rev. Lett. **53**, 878 (1984); S. Ono, N. Törnqvist, J. Lee-Franzini, and A. Sanda, Phys. Rev. Lett. **55**, 2938 (1985); S. Ono, A. Sanda, and N. Törnqvist, Phys. Rev. D **34**, 186 (1986).
[4] M. Artuso *et al.* (CLEO Collaboration), Phys. Rev. Lett. **95**, 261801 (2005).
[5] G. Bonvincini *et al.* (CLEO Collaboration), Phys. Rev. Lett. **96**, 022002 (2006).
[6] E. Eichten *et al.*, Phys. Rev. D **21**, 203 (1980).
[7] D. Peterson *et al.*, Nucl. Instrum. Methods Phys. Res., Sect. A **478**, 142 (2002); M. Artuso *et al.*, Nucl. Instrum. Methods Phys. Res., Sect. A **554**, 147 (2005); Y. Kubota *et al.*, Nucl. Instrum. Methods Phys. Res., Sect. A **320**, 66 (1992).
[8] G. C. Fox and S. Wolfram, Phys. Rev. Lett. **41**, 1581 (1978).
[9] S. Eidelman *et al.*, Phys. Lett. B **592**, 1 (2004) and 2005 partial update for the 2006 edition available on the PDG WWW pp. (http://pdg.lbl.gov/).
[10] S. E. Csorna *et al.* (CLEO Collaboration), Phys. Rev. D **67**, 112002 (2003).
[11] For this decay, the helicity angle $\theta_h$ is the angle between the $\pi^0$ direction in the $\rho$ rest frame and the $\rho$ direction in the $D$ rest frame.
[12] T. Sjöstrand *et al.*, Comput. Phys. Commun. **135**, 238 (2001).
[13] QQ—The CLEO Event Generator, http://www.lns.cornell.edu/public/CLEO/soft/QQ.
[14] E. Barberio and Z. Was, Comput. Phys. Commun. **79**, 291 (1994).
[15] R. Brun *et al.*, GEANT 3.21, CERN Program Library Long Writeup W5013 (unpublished), 1993.
[16] The $B^*$-$B$ mass difference is $45.78 \pm 0.35\ \mathrm{MeV}/c^2$, to which a $1.7\ \mathrm{MeV}/c^2$ Lorentz boost correction was applied that reflects our use of the $B$ meson momentum in computing $M_{\rm bc}$ rather than the $B^*$ momentum.
[17] G. Feldman and R. Cousins, Phys. Rev. D **57**, 3873 (1998).
[18] This value is reduced by the beam energy correction of 4.6 MeV which was applied in Ref. [5].
[19] D. Acosta *et al.* (CDF Collaboration), hep-ex/0508022.
[20] J. Lee-Franzini *et al.* (CUSB Collaboration), Phys. Rev. Lett. **65**, 2947 (1990).
[21] W. Bardeen, E. Eichten, and C. Hill, Phys. Rev. D **68**, 054024 (2003), and references therein.